

Gain, nonlinearity and regulation in the mammalian cochlea

ROBERT B. PATUZZI¹, AND GREG A. O'BEIRNE^{1,2}

¹ *The Auditory Laboratory, Discipline of Physiology, The University of Western Australia, Crawley, Australia*

² *Department of Communication Disorders, University of Canterbury, Christchurch, New Zealand*

Apart from acute conductive problems, we normally think of a person's pure-tone audiogram as relatively fixed, changing rapidly only rarely (e.g. stroke, fistula, Ménière's syndrome). Given that outer hair cells (OHCs) actively enhance cochlear vibration 50-60dB by cancelling internal friction, we should expect cochlear gain to be very sensitive to changes in component parts, as in any positive feedback system. This is especially true when the components are highly nonlinear, with their small-signal efficiency depending on the slope of their transfer curve at the operating point. As a result, it seems inescapable that cochlear gain is regulated in some way. Indeed there *is* evidence that it is usually maintained within a tolerance of a few decibel by good 'design' to reject disturbances, and by a dynamic servo-loop to stabilize gain. For example, after intense but non-traumatic low-frequency tones, the audiogram can slowly oscillate up and down by as much as 30 dB, suggesting underdamped gain stabilization. How the cochlea's design minimizes large perturbations and how OHCs stabilize their gain are discussed using experimental data from animals and humans, and with mathematical modelling of the feedback systems controlling the highly nonlinear OHCs. This suggests that co-evolution of the cochlea's geometry, electro-anatomy and membrane proteins has produced a robust system to stabilize the OHC feedback forces against changes in the cochlea's internal battery (endocochlear potential), against slow changes in pressure within the cochlea, and ultimately against unavoidable variations in the density of the OHC's own membrane proteins.

INTRODUCTION

The sensitivity and frequency selectivity of the normal mammalian cochlea is quite extraordinary (Patuzzi and Robertson, 1988), and largely due to the sensitive and complex vibration of the organ of Corti (Patuzzi, 1996; Robles and Ruggero, 2001). From animal experiments that disrupt hair cell processes *in vivo* and *in vitro*, and from the existence and nonlinearity of otoacoustic emissions (OAEs) in animals and humans, it is clear that the mammalian outer hair cells (OHCs) are electromotile, and apply electromechanical (positive) feedback that cancels internal friction. This positive feedback enhances mechanical and neural sensitivity by 50-60 dB. While there is still debate about whether the dominant force generator assisting vibration is the electromotile prestin packed densely in the OHC basolateral wall (Zheng *et al.*, 2000), or other processes directly associated with the mechano-electrical (MET) process at the hair bun-

dle (Eatock, 2000), what is not in doubt is that both the forward mechano-electrical transduction (MET; from movement to ionic current) and reverse electro-mechanical transduction (EMT; from ionic current to feedback forces) are highly nonlinear and labile. This reliance on positive feedback makes the system extremely dependent on the efficiency or tolerance of components in the signal path. The nonlinearity of these components makes it relatively easy for large (slow) disturbances to produce partial saturation, and therefore significant changes in active gain (and two-tone interactions like two-tone suppression and distortion generation). For example, a 20% drop in the efficiency of OHC MET produces a 10-fold (20 dB) drop in the vibration of the organ of Corti near its resonance frequency (Patuzzi *et al.*, 1989) and a 20 dB elevation of neural threshold (Fig. 1C). Open-loop efficiency of OHC MET was estimated from maximal round-window CM at 200 Hz (horizontal axis), because in the cochlear base at 200 Hz OHC active assistance is irrelevant. Active gain at the same location was estimated neurally from mean compound action potential (CAP) thresholds for tonebursts at 10-20 kHz, where OHC assistance is crucial. Data were obtained by disrupting OHC MET with multiple traumatic 10 kHz tones (20 animals). We can assume that any disruption of *overall efficiency* around the feedback path would produce similar changes. For example, if the input variable to a component in the signal path were I , and the output variable were O , then its small-signal efficiency would be $\eta(O)=dO/dI$ (the slope of the component's nonlinear transfer function at its operating point). With n components in cascade, the overall small-signal efficiency through the cascade would be $\eta_{tot} = \eta_1 \cdot \eta_2 \cdot \eta_3 \dots \eta_n$, and system gain would depend on η_{tot} via a sensitivity function, $S(\eta_{tot})$, and on the operating point on each component's transfer curve. Fig. 1C suggests empirically that the link between open-loop small-signal efficiency (η_{tot}) and loss of overall cochlear gain in decibel (hearing loss, HL) is given by $HL(dB)=101dB \cdot (1-\eta_{tot})/[1+0.85(1-\eta_{tot})]$. For the mammalian cochlea to reliably detect sound with a tolerance less than 5dB (smallest step on a clinical audiogram), it clearly must rely on two 'design' strategies to reduce everyday gain fluctuations to less than 5%. First, the structures of the middle and inner ear must ensure that any large slow disturbances (operating point shifts) are minimized by: (i) a coiled cochlear structure in hard (non-compliant) temporal bone, (ii) optimised cross-sectional areas of scala tympani and scala vestibuli to null common-mode stimulation through bone-conduction, (iii) a Eustachian tube to minimize tympanum displacements with slow air pressure changes, (iv) a slip joint at the malleo-incudal joint to further minimize stapes displacements, (v) an helicotrema to equalize perilymphatic pressures if large and slow stapes displacements do occur, and (vi) viscously-coupled hair bundles on inner hair cells to avoid direct stimulation of neurones during any slow disturbance. Second, the combination of ion transport and two types of cell motility in OHCs must produce autoregulation when slow disturbances are not fully rejected by the measures above. In particular, ion transport proteins in the OHC basolateral wall must stabilize the electrical potential within these cells, and their contractility must regulate their hair bundle angle and MET efficiency, as described later.

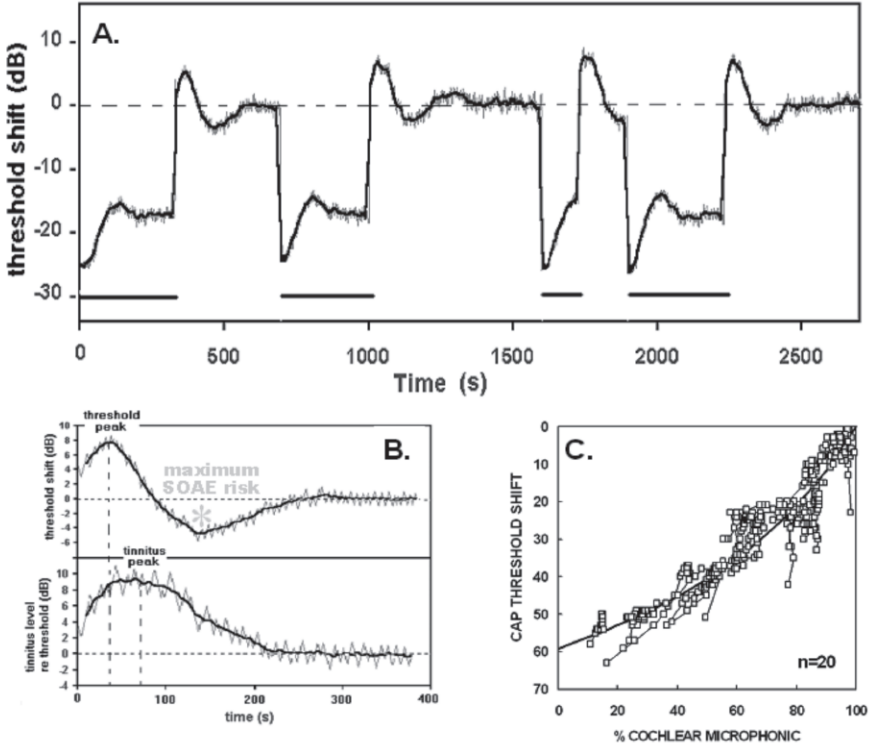


Fig. 1: (A) Slow oscillations in human threshold at 2.5kHz during (black bars) and after intense 40Hz tones (126dB SPL). Note hypersensitive 'bounce' 2 minutes after each tone (unsmoothed Bekey thresholds, grey trace). (B) 1.3kHz human threshold oscillating after LF exposure (upper panel) and change in tinnitus level associated with it (lower panel). Note best threshold and peak tinnitus do not coincide. (C) Mean threshold shift (10-20kHz) versus drop in 200Hz round-window CM in 20 guinea pigs after 10kHz overstimulation (115dB SPL).

The 'bounce' phenomenon as perturbed autoregulation of cochlear gain from OHCs

One phenomenon often called 'the bounce' provides insight into cochlear gain regulation. It is the very low frequency (VLF) oscillation in hearing threshold just after a few minutes exposure to an intense but non-traumatic low-frequency (LF) tone. After such a tone, auditory thresholds are initially elevated (Fig. 1A) but then recover in a non-monotonic way. They improve over a minute or more, so that at 2 minutes they are sometimes better than normal (arrow, Fig. 1A), but then worsen again in a damped oscillation (period 150-230 s, depending on audiometric frequency), before settling after about 10 minutes. Hirsh and Ward (1952) originally referred to the worsening of thresholds *after* 2 minutes as the 'bounce' (asterisk, Fig. 1A), although more recently others (Kemp, 1986; Kirk & colleagues, 1997) have focused on the first hypersensitivity (arrow, Fig. 1A). Some fundamental features of this bounce can be studied with

human psychophysical experiments, including the transient tinnitus associated with it (Zwicker and Hesse, 1984; Patuzzi and Wareing, 2002; Patuzzi and Wareing, in preparation). Overall, the psychophysical experiments indicate the following:

- (a) The bounce is a damped sinusoid, indicating an underdamped servo-loop controlling gain (a view consistent with its enhancement by well timed LF bursts; Zwicker and Hesse, 1984).
- (b) The bounce's VLF is different at each CF region (from 150-230s period as probe frequency rises) indicating a local mechanism (i.e. not a global cochlear oscillation as in fluid pressure).
- (c) LF tones above about 500Hz are ineffective in evoking a bounce, so that the input to the VLF resonator formed by the under-damped servo-loop seems low-pass filtered (LPF).
- (d) A change of LF tone frequency does not change the bounce's VLF at each CF site, suggesting that the input is converted to an equivalent DC step input (i.e. rectified).
- (e) There is saturation of bounce amplitude at high SPLs (regardless of LF stimulus), suggesting that the input to the VLF servo-loop resonator clips.
- (f) Onset- and offset-bounces are inverted, but have approximately equal amplitude and frequency (Fig. 1A), indicating that the VLF servo-loop is not itself driven into saturation.
- (g) Bounce amplitude is greater at lower CF regions (the more compliant cochlear apex), indicating that the drive to the VLF resonator is displacement of the organ of Corti.
- (h) The bounce phase is not zero. Maximum and minimum gains do not coincide with the tone onset and offset, indicating a phase delays between the input and the gain-control element/s.
- (i) The tinnitus with the bounce does not peak at the same time as the gain (gain at tinnitus peak about normal, Fig. 1B). That is, the tinnitus is not simply hypersensitivity of cochlear gain.

These observations allow a first guess at the system controlling cochlear gain at each CF region (Fig. 2A). The LF tone input produces a LF displacement of the organ of Corti (larger in the apex due to higher compliance), which then produces an intermediate response that appears to be clipped and then low-pass filtered at about 500Hz. This intermediate is likely to be the large saturating AC receptor potential within the OHCs, low-pass filtered by the OHC's membrane impedance (itself dominated by membrane capacitance at higher frequencies). The rectifier/filter transforming the large AC receptor potential to a DC step applied to the gain control servo-loop is likely to be the rectified Ca^{2+} entry into these cells, where Ca^{2+} channels are opened during the depolarizing half-cycle of the AC receptor potential, but are closed during its hyperpolarizing

half-cycle. The net result is a step rise in OHC cytosolic Ca^{2+} during low-frequency stimulation, but, as discussed below, Ca^{2+} sequestration and other ion transport mechanisms in OHCs produce a damped oscillation in intracellular Ca^{2+} , which oscillates slowly and modifies OHC properties (e.g. membrane potential, cell length, hair bundle angle, basolateral conductance). Two crucial questions are which OHC variable/s and what mechanism/s are responsible for the dominant modulation of cochlear gain (there may be more than one). These questions are not just relevant to the mechanism of the bounce, but address the origin of masking in the normal and abnormal human ear, and the mechanisms producing sensorineural hearing loss when autoregulation fails (possibly in Ménière's syndrome).

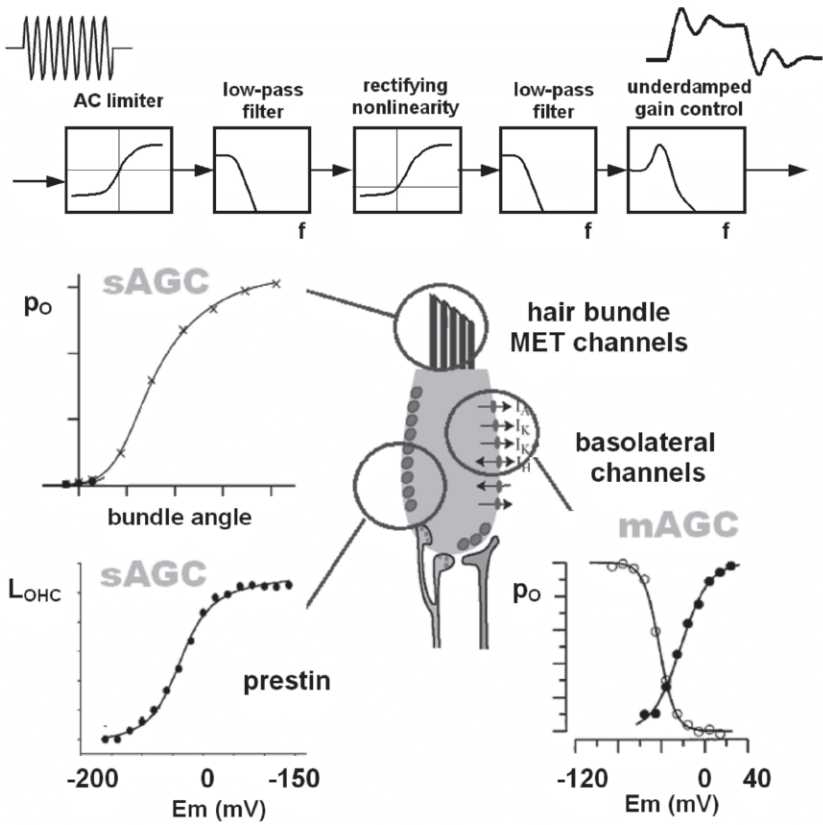


Fig. 2: (Top) Block diagram of system producing slow oscillation in cochlear gain (see text). (Bottom) Main nonlinearities in OHC transduction, each a possible site of gain modulation.

Mechanisms of automatic gain control (AGC)

In electronic circuits (especially those involving positive feedback to enhance gain) there are three simple methods of automatic gain control (AGC; Fig. 3): (i) saturation feedback, where a nonlinearity in a positive feedback path (symmetrically) clips the AC feedback signal at high signal levels, reducing net gain (Zwicker, 1979; as in the amplitude stabilization of a Wien bridge oscillator); (ii) multiplicative-AGC (mAGC) where the output signal is used to derive a DC control (by rectification and low-pass filtering) that parametrically controls a multiplier element in the signal path (often a simple shunt element, and with an exponential attack and decay time); and (iii) gradient- or slope-AGC (sAGC), where a similar DC control signal is used to move the operating point on the nonlinear transfer function of a crucial element in the feedback or signal path, thereby altering the element’s small-signal efficiency. In sAGC it is sometimes necessary to high-pass filter the output signal to remove the signal component associated with the DC control signal. Such mAGC and sAGC are used in tremolo circuits in guitar amplifiers and simple AM modulators in audio and RF circuits.

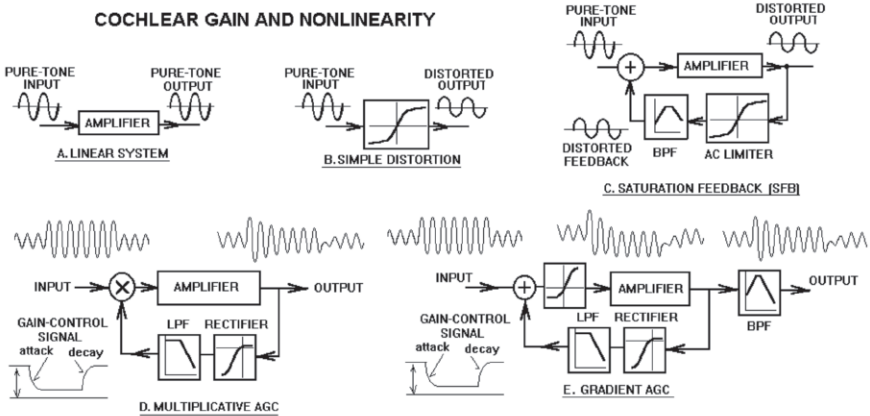


Fig. 3: (A) Linear system with no distortion. (B) Simple distortion in system with no feedback. (C) Symmetric clipping in a positive feedback path provides AGC through 'saturation feedback'. (D) Rectification and smoothing of system output to produce a DC gain-control signal that alters gain by simple multiplication (often a signal shunt) via multiplicative-AGC (mAGC). (E) As in (D), but gain control achieved by altering operating point on nonlinear transfer curve via gradient- or slope-AGC (sAGC). The DC control signal can be removed by high-pass filtering.

The existence of such nonlinearities in a system can often manifest as intermodulation, including distortion product generation and two-tone interference or two-tone-suppression, where a ‘suppressor’ tone reduces the system’s output to another ‘probe’ tone. If the suppressor tone is at a low-frequency, the modulation of the probe tone can be seen cycle-by-cycle, and the process is called either low-frequency biasing or, in psychophysics, a “masking period pattern” (Zwicker, 1976, 1979). Designers of analog circuits know well that a nonlinearity in the signal path can produce a loss of gain if the nonlinearity is biased to an insensitive (shallow-sloped) part of its transfer func-

tion. Manufacturers of guitar amplifiers used the nonlinearity of convenient components (valves, diodes, transistors and even light globes) to produce a tremolo feature by using a low-frequency oscillator to drive a nonlinear component cyclically into partial saturation. In badly designed audio power amplifiers, excessive circuit current can slowly drain the power supply, causing inadvertent feedback from power supply to amplifier, causing the system to oscillate at a very low frequency, producing a repetitive and loud thumping in the speakers known as "motor-boating". If the oscillation is sufficiently slow it may be inaudible, but it manifests as a slow cyclic rise and fall in the hiss level from the speakers as the oscillation modulates circuit noise by the cyclic saturation of a dominant nonlinearity in the signal path. This disconcerting periodic hiss is known as "breathing". A similar phenomenon occurs in human hearing when driving at high speed with one window partly down. The combination of the small window aperture and the large cab produces a subsonic Helmholtz resonance at 7-15Hz. Wind past the window causes the car to oscillate like a subsonic flute, cyclically biasing the nonlinear OHCs into saturation twice per cycle (on peak positive and negative excursions; Patuzzi *et al.*, 1984, 1989), modulating hearing threshold to produce 'fluttering' or 'chopped' hearing, and Zwicker's masking period patterns. The dominant nonlinearity in the signal path appeared to be the OHC MET transfer curve (Patuzzi *et al.*, 1989), but nonlinear prestin motility may contribute. Moreover, as the intensity of the low-frequency masker increases, there is not only a deepening of the cyclic modulation of cochlear gain, but an overall loss of gain (Patuzzi *et al.*, 1982), suggesting the combination of both fast and slow sAGC and mAGC mechanisms.

Investigating regulation of cochlear gain with in vivo experiments and cell modelling

We have studied the bounce phenomenon and cochlear gain regulation in two ways. First, we have perturbed cochlear regulation and observed as many cochlear indicators as we can (using psychophysical threshold tracking in humans and electrocochleographic indicators in guinea pigs). Second, just as circuit performance in electronics can be studied with simulation programs such as SPICE, we can combine the known OHC membrane transport proteins and motile mechanisms to model their dynamic behaviour in response to large perturbations. By comparing these simulations with in vivo and psychophysical experiments we can gain an insight into which variables and nonlinearities are important in controlling cochlear gain.

Monitoring OHC behaviour with the low-frequency cochlear microphonic potential (CM)

Rather than simply using the magnitude of the CM as an indicator of OHC receptor current (Fig. 1A), we have also analysed the distorted CM waveforms in detail, to extract as much information as possible (Patuzzi and Molerinho, 1998; Patuzzi and O'Beirne, 1999). By plotting the distorted CM against the presumed sinusoidal mechanical drive to the OHC hair bundles, we can create a Lissajous figure (Fig. 4), which reconstructs the nonlinear MET transfer function relating displacement of OHC hair bundles to OHC receptor current (which flows through the cells into scala tym-

pani, producing the extracellular CM). By curve-fitting to this Lissajous figure we can extract three important parameters: (a) the equivalent operating point (E_o) on the non-linear MET transfer curve (horizontal shift along the displacement axis, which indicates equivalent hair bundle angle); (b) the maximal receptor current amplitude (V_{sat}) when all MET channels are cyclically opened and closed (proportional to the number of OHCs contributing to the CM, the number of MET channels active in this OHC population, the conductance of the OHC basolateral wall, itself determined by intracellular Ca^{2+} , and the total driving potential for flow of OHC transduction current, which is the endocochlear potential (EP) minus the OHC membrane potential); and (c) the net sensitivity (Z) of the MET process (maximum slope of vertically normalized transfer curve, which we presume to be proportional to the equivalent compliance of the organ of Corti). With a fast computer these three MET parameters can be extracted in real-time from the distorted CM, allowing a determination of which OHC variable/s best correlates with the changes in cochlear gain during a bounce. Because we can simultaneously monitor the EP in our animal experiments using glass micropipettes in scala media, we are also able to determine whether any changes in V_{sat} are consistent with a change in EP, or a change in the conductance of the OHC basolateral wall (and presumably due to changes in intracellular Ca^{2+}). For example, if V_{sat} rises as EP falls then the V_{sat} change is probably due to a rise in OHC basolateral conductance. This ability to monitor multiple OHC properties during a bounce allows us to exclude some OHC processes as the cause, as described later.

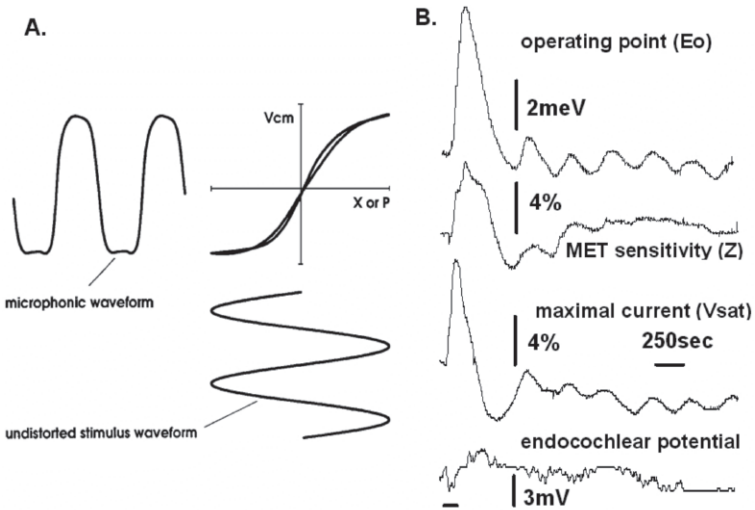


Fig. 4: (A) An intense 200Hz tone produces distorted CM at the guinea pig round-window. Plotting CM against sinusoidal input produces a Lissajous figure representing the MET transfer curve. (B) Curve-fitting to such curves allows extraction of OHC parameters (see text), and electrodes in scala media measure EP. Here the perturbation was a small step rise in perilymph pressure due to a poor experimental perfusion.

Modelling the role of OHC ion transport and motility in autoregulating cochlear gain

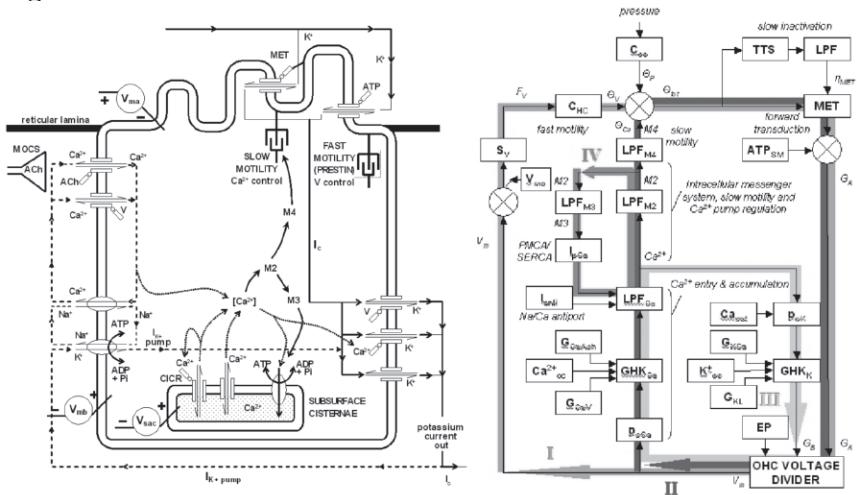


Fig. 5: (A) A mathematical model of OHC behaviour can be constructed by considering some known ion transport pathways in these cells, and two forms of cell motility (see text). (B) Such models highlight four main feedback loops within OHCs that might regulate cochlear gain.

We have described our OHC modelling process in detail elsewhere (O’Beirne and Patuzzi, in press). In essence, we have included two motile mechanisms in the OHC model: a slow Ca²⁺-dependent motility (Farahbakhsh and Narins, 2006) and a voltage-dependent fast-motility (prestin; Zheng *et al.*, 2000). We have also assumed that prestin is the main force-generating component of the high-frequency active process (Zheng *et al.*, 2000). We have not included electromotility from the stereocilia or hair bundle adaptation (Eatock, 2000), to see how much of our experimental data can be explained without them. The model OHC also has an apical membrane with MET (Holton and Hudspeth, 1986) facing scala media and bathed in endolymph, and a basolateral membrane facing perilymph that contains the known ion transport proteins in OHCs (Housley and Ashmore, 1992), including voltage-controlled Ca²⁺ channels, a Ca²⁺ extrusion process (an antiport), and Ca²⁺-controlled K⁺ channels that can open to partially short the voltage across the basolateral wall. The cell interior is itself divided into two compartments: the subsurface cisternae that form an intracellular Ca²⁺ store, and the cytosol bathing them, which has changing concentrations of Ca²⁺ and three putative biochemical messengers (M2, M3 and M4) in a second messenger cascade (see also Frolenkov *et al.*, 2000, 2006). In the model, a rise in Ca²⁺ increases M2, which increases M3 and M4. A rise in M3 accelerates Ca²⁺ sequestration, while M4 causes slow OHC contraction. This putative messenger system accounts for many of our experimental observations by introducing phase delays between any change in cytosolic Ca²⁺ and its action on the M4-dependent slow-motility, the Ca²⁺-dependent conductances, and the accelerated removal of Ca²⁺ from the cytosol by the M3-con-

trolled transport proteins. Together this system (Fig. 5A) forms the OHC’s complex autoregulation system, normally stabilizing OHC membrane potential and MET operating point (and therefore sAGC and mAGC gains; Fig. 4). Moreover, the phase delays in the $\text{Ca}^{2+}/\text{M2}/\text{M3}\&\text{M4}$ cascade can cause the OHC Ca^{2+} and the Ca^{2+} -dependent properties to slowly oscillate after perturbations, as in the ‘bounce’.

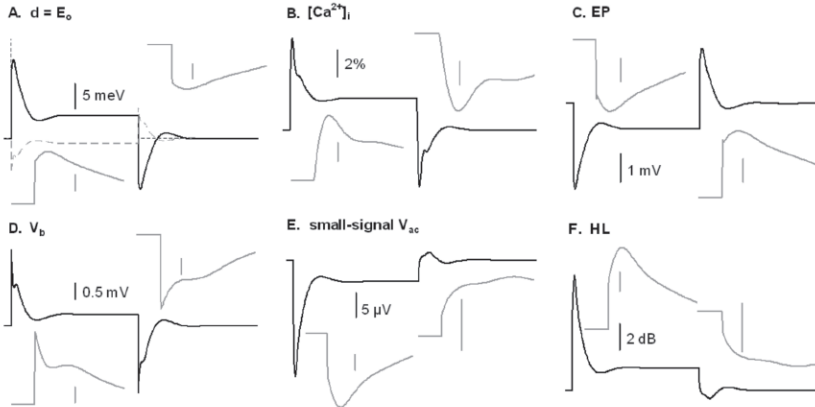


Fig. 6: Modelling of OHC ion transport and cell motility predicts the time course of important OHC variables after perturbations. (A) hair bundle displacement, (B) cytosolic Ca^{2+} , (C) endocochlear potential, (D) membrane potential, (E) small-signal AC receptor potential, and (F) loss of cochlear gain. These examples were produced by a small step increase in scala tympani pressure, and demonstrate oscillation modes similar to ‘the bounce’. Black curves are over 60 minutes, while grey curves show detail of the onset and offset over 5 minutes.

Figure 5B shows the resulting four main negative feedback loops in OHCs (shaded arrows labelled I to IV). To demonstrate the influence of these feedback loops, consider the application of a positive hydrostatic pressure bias to scala tympani. First, the pressure stimulus would (following Feedback Loop I): (i) move MET operating point towards scala vestibuli; (ii) increase apical conductance via the MET channels; (iii) depolarise the cells via the cell voltage divider; (iv) shift MET operating point more with prestin, counteracting the initial operating point shift. Following Feedback Loop III, the depolarisation (point iii above) would: (v) activate basolateral voltage-sensitive Ca^{2+} channels and cause Ca^{2+} influx; (vi) raise cytosolic Ca^{2+} due to the elevated influx; (vii) activate basolateral Ca^{2+} -sensitive K^{+} channels, producing hyperpolarization; (viii) open voltage-sensitive basolateral K^{+} channels, counteracting the depolarisation above. Following Feedback Loop IV, the increased cytosolic Ca^{2+} concentration (point vi) would: (ix) increase Ca^{2+} efflux through basolateral antiports; (x) activate intermediate M2 and so intermediate M3; (xi) speed Ca^{2+} sequestration via the M2/M3 cascade, (xii) with the Ca^{2+} antiport efflux and sac sequestration summing to produce a drop in cytosolic Ca^{2+} ; counteracting the rise in cytosolic Ca^{2+} (point vi). Finally (Feedback Loop II), a rise in M2 (point x above) would: (xiii) increase M4, causing cell contraction via slow motility, producing a scala tympani operating point

shift, counteracting the initial operating point shift. In other words, these feedback loops can buffer the cell against perturbations, providing some autoregulation, and can be described in physiological terms as “homeostatic”. However with large phase delays and excessive gain such a system is susceptible to oscillations. Examples of the response of the model to a small step increase in scala tympani fluid pressure is shown in Fig. 6. Although these particular responses were from a simplified model without nonlinear prestin and which was not optimised to produce a ‘bounce’, they illustrate that slow oscillations are possible. Fig. 7 also illustrates that such models can predict the ability of these cell mechanisms to stabilize key OHC variables, most notably MET operating point and membrane potential, using cytosolic Ca^{2+} as the major control variable. In the case of the bounce, the step perturbation is likely to be caused by an intense LF tone which causes a large AC receptor potential and a rectified Ca^{2+} entry, which presents the underdamped Ca^{2+} regulation mechanism with a step Ca^{2+} increase. This Ca^{2+} rise and oscillation then cause a similar (but phase-delayed) oscillation in MET operating point, membrane potential, and cytosolic Ca^{2+} and therefore basolateral conductance, and all modify cochlear gain via mAGC and sAGC processes.

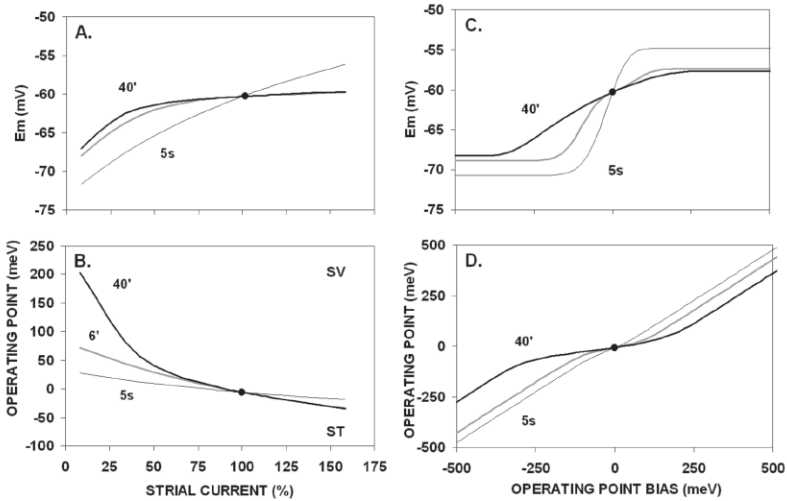


Fig. 7: (A) Sample OHC ‘regulation curves’ (5s, 6’ and 40’ after onset of perilymphatic pressure rise), obtained by plotting magnitude of a key OHC variables (here membrane potential top and MET operating point bottom) against magnitude of a disturbance (here change in strial current [A & B] or perilymphatic pressure [C & D]). Mechanisms included in the model stabilized OHCs.

Finally, the precarious combination of positive feedback and component nonlinearity could have been the mammalian ear’s downfall, with everyday disturbances able to partially saturate OHC components and produce hearing loss. However the simultaneous evolution of structures to reduce the disturbances, and of autoregulation to keep key OHC variables within their operating range, allowed this precarious assemblage

of proteins to function remarkably well (in most cases). The successful convergence of these aspects of mammalian hearing is unlikely to have been by luck or divine intervention: the consequences of failure in autoregulation would have been (and still are) a fluctuating audiogram and tinnitus. That is, the price of failure was so high that success was not just possible, but almost inevitable as random mutations of the failed Cl- transporter prestin finally matched prestin's properties to the probably pre-existing and regulated OHC environment (see Franchinia and Elgoyhena, 2006).

REFERENCES

- Eatock, R. A., (2000). "Adaptation in hair cells," *Annual Review of Neurosci.* **23**, 285-314.
- Farahbakhsh, N. A. Narins, P. M., (2006). "Slow motility in hair cells of the frog amphibian papilla: Ca²⁺-dependent shape changes," *Hear. Res.* **212**:140–159.
- Franchinia, L. F., and Elgoyhena, A. B., (2006). "Adaptive evolution in mammalian proteins involved in cochlear outer hair cell electromotility". *Molecular Phylogenetics and Evolution* **41**, 622-635.
- Frolenkov, G. I., (2006). "Regulation of electromotility in the cochlear outer hair cell," *J. Physiol.* **576**, 43-48.
- Frolenkov, G. I., Mammano, F. Belyantseva, I. A., Coling, D., Kachar, B., (2000). "Two distinct Ca²⁺-dependent signaling pathways regulate the motor output of cochlear outer hair cells," *J. Neurosci.* **20**, 5940–5948.
- Holton, T., Hudspeth, A. J., (1986). "The transduction channel of hair cells from the bull-frog characterized by noise analysis," *J. Physiol. (Lond.)*, **375**, 195-227.
- Housley, G. D., Ashmore, J. F., (1992). "Ionic currents of outer hair cells isolated from the guinea-pig cochlea," *J. Physiol. (Lond.)*, **448**, 73-98.
- Kemp, D. T., (1986). "Otoacoustic emissions, travelling waves and cochlear mechanisms," *Hear. Res.* **22**, 95-104.
- Kirk, D. L., Moleirinho, A., and Patuzzi, R. B., (1997) "Microphonic and DPOAE measurements suggest a micromechanical mechanism for the 'bounce' phenomenon following low frequency tones," *Hear. Res.*, **112**, 69-86.
- Kirk, D. L., Patuzzi, R. B., (1997). "Transient changes in cochlear potentials and DPOAEs after low-frequency tones: the 'two-minute' bounce revisited," *Hear. Res.* **112**, 49-68.
- O'Beirne, G. A., Patuzzi, R. B., (2003). "Mathematical modelling of the role of outer hair cells in cochlear homeostasis," *Biophysics of the Cochlea*. World Scientific, Singapore, 434-435.
- O'Beirne, G. A., Patuzzi, R. B., (2007). "Mathematical model of outer hair cell regulation including ion transport and cell motility," *Hear. Res.* (in press).
- Patuzzi, R., (2002). "Outer hair cells, EP regulation and tinnitus," in. *Proceedings of the Seventh International Tinnitus Seminar*. University of Western Australia, Crawley, 16-24.
- Patuzzi, R., and Sellick, P. M., (1984). "The modulation of the sensitivity of the mammalian cochlea by low frequency tones. II. Inner hair cell receptor potentials," *Hear. Res.* **13**, 9-18

- Patuzzi, R., and Robertson, D. (1988). "Tuning in the mammalian cochlea," *Physiol. Rev.* **68**, 1009-1082.
- Patuzzi, R., Sellick, P. M., and Johnstone, B.M., (1984) "The modulation of the sensitivity of the mammalian cochlea by low frequency tones. III. Basilar membrane motion", *Hear. Res.* **13**, 19-27.
- Patuzzi, R., Sellick, P. M., Johnstone, B. M., (1984). "The modulation of the sensitivity of the mammalian cochlea by low frequency tones. I. Primary afferent activity," *Hear. Res.* **13**:1-8.
- Patuzzi, R., Wareing, N., (2002). "Generation of transient tinnitus in humans using low-frequency tones and its mechanism," in *Proceedings of the Seventh International Tinnitus Seminar*. University of Western Australia, Crawley, 71-73.
- Patuzzi, R. B., (1996). "Cochlear micromechanics and macromechanics," in *The Cochlea*. Springer-Verlag, New York, NY, pp. 186-257.
- Patuzzi, R. B., (2003). "Low-frequency oscillations in outer hair cells and homeostatic regulation of the organ of Corti," in *Biophysics of the Cochlea*. World Scientific, Singapore, 292-299.
- Patuzzi, R. B., O'Beirne, G.A., (1999). "Boltzmann analysis of CM waveforms using virtual instrument software," *Hear. Res.*, **133**, 155-159.
- Patuzzi, R. B., Yates, G. K., and Johnstone, B. M., (1989). "Outer hair cell receptor current and sensorineural hearing loss", *Hear. Res.* **42**, 47-72.
- Robles, L., Ruggero, M. A., (2001). "Mechanics of the Mammalian Cochlea," *Physiol. Rev.* **81**, 1305-1352.
- Sellick, P. M., Patuzzi, R., and Johnstone, B. M., (1982). "Modulation of responses of spiral ganglion cells in the guinea pig cochlea by low frequency sound," *Hear. Res.* **7**, 199-221.
- Zheng, J., Shen, W., He, D.Z., Long, K.B., Madison, L.D., Dallos, P., (2000). "Prestin is the motor protein of cochlear outer hair cells," *Nature* **405**, 149-155.
- Zwicker, E. (1976). "Psychoacoustic equivalent of period histograms [in memoriam Dr. Russell Pfeiffer]," *J. Acoust. Soc. Am.*, **59**, 166-175.
- Zwicker, E. (1979). "A model describing nonlinearities in hearing by active processes with saturation at 40 dB," *Biological Cybernetics*, **35**, 243-250.
- Zwicker, E., Hesse, A., (1984). "Temporary threshold shifts after onset and offset of moderately loud low-frequency maskers," *J. Acoust. Soc. Am.* **75**, 545-549.

